# Chapter 6
# Ambient Noise in the Canadian Arctic

**Emmanuelle Cook, David Barclay, and Clark Richards**

**Abstract** Numerous studies of ocean ambient noise and under-ice acoustic propagation and reverberation in the Canadian Arctic have been carried out since the 1960s. These studies, largely led by scientists at the Defence Research Establishment Pacific and Defence Research and Development Canada, have been motivated by the need to improve sonar performance prediction in the Arctic over the wide range of seasonal ice, oceanographic, and meteorological conditions at high latitudes. Aside from the valuable insight into the physics of noise generation by sea ice and sound propagation under sea ice, they provide a historical baseline for Arctic ambient noise against which modern measurements can be compared. In 2017, the Department of Fisheries and Oceans added passive acoustic monitoring to their Barrow Strait Real Time Observatory, reporting power spectral density over the acoustic band of 10–800 Hz in 2017–2018 and 10–6400 Hz in 2018–2019. Co-located measurements of ice draft, salinity, temperature, and current profiles, along with nearby meteorological measurements, provide time series of environmental forcing and conditions. An updated seasonal baseline for ambient noise in Barrow Strait is calculated and compared against historical measurements, along with a review of noise-generating mechanisms and transmission loss models in the Arctic.

**Keywords** Acoustic propagation · Ambient noise · Arctic soundscape · Under-ice propagation

E. Cook · D. Barclay (✉)
Department of Oceanography, Dalhousie University, Halifax, Canada
e-mail: emmanuellecook@dal.ca; dbarclay@dal.ca

C. Richards
Bedford Institute of Oceanography, Fisheries and Oceans Canada, Halifax, Canada
e-mail: clark.richards@dfo-mpo.gc.ca

## 6.1    Introduction

The Arctic Ocean is the northernmost body of water in the world and features constant ice cover, causing temperature and salinity profiles unlike any other ocean basin. These unique profiles keep cool freshwater at the surface and, together, generate a unique sound speed profile which has a positive gradient with increasing depth causing horizontally propagating sound waves to be refracted towards the surface. This has the effect of creating a shallow sound channel, shown in Fig. 6.1, allowing sound to travel great distances where the primary loss mechanism is due to the sea ice itself (Hutt 2012).

Ice cover also makes the Arctic Ocean difficult to access. However, the low levels of anthropogenic noise make it ideal for studying the myriad of natural sound sources that contribute to underwater noise levels. With receding ice cover due to climate change, existing shipping channels are becoming accessible for greater periods of the year, and new channels will begin to open, allowing ship traffic to increase. In fact, shipping in the Arctic has tripled over the past 20 years (Giesbrecht 2018), and with this increase comes the growing concern of its effects on marine life, including the impact of ship-generated noise on the underwater soundscape (Stephenson et al. 2011).

Thus, quantifying the natural ambient noise levels of the Canadian Arctic Ocean is becoming increasingly important in order to establish a baseline for this environment. The mechanisms of natural ambient noise generation must be understood in order to accurately model and predict the background against which increasing the sounds of anthropogenic activity (noise pollution) will be added to the marine habitat. In order to model the temporal and spatial extent of both natural and human-generated noise, the transmission of underwater sound in the unique Arctic waters must be understood. Several models have proposed methods to capture the
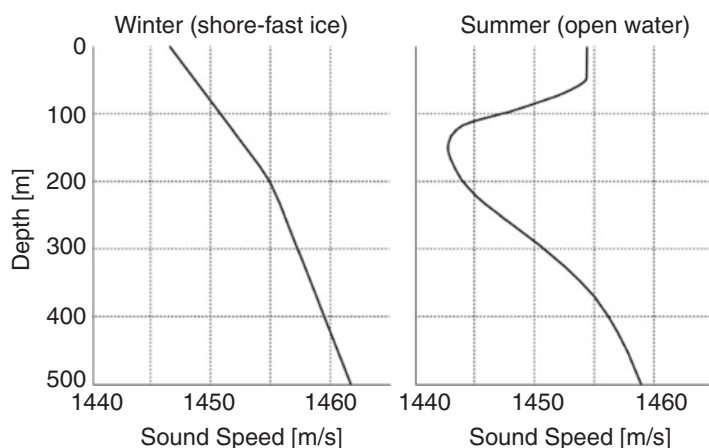


**Fig. 6.1** Typical sound speed profiles in the Arctic, demonstrating the under-ice surface duct in winter and the shallow sound channel at 150 m in summer (Hutt 2012)

transmission losses associated with sea ice: shear energy conversion, rough water-ice interface scattering, and scattering and shadowing by large ice keels.

This chapter will give a brief summary on ambient noise studies that have been conducted in the Arctic with an emphasis on presenting research conducted in the Canadian Arctic. So far, studies have described a few dominant noise-generating mechanisms in the Arctic, ice combined with wind and temperature changes being the leading ones (Urick 1984; Carey and Evans 2011; Hutt 2012). Recent work on the use of permanent monitoring systems for the real-time reporting of ambient noise is presented.

## 6.2  Survey of Acoustic Measurements

A variety of techniques have been used for measuring ambient noise levels in the Arctic Ocean. They have ranged from single hydrophones to hydrophone arrays that are lowered from ice stations, drifting buoys, and moored or mounted to the sea floor. Experimental interest has been primarily focused on the effects of the shallow propagation channel and the rough ice surface on ambient noise properties. Consequently, measurements conducted in the Arctic have generally been made in the littoral zone (< 300 m) and over low-frequency bands (10–1000 Hz). In this section, a summary of ambient noise measurements in the Canadian Arctic is presented historically, by region and by experimental method.

### 6.2.1  Temporal Distribution of Measurements

Arctic ambient noise has been studied in Canada since the mid-1900s. Measurements before the 1990s were usually conducted in the spring and summer months due to both the difficulty of access caused by ice cover and the harsh weather conditions in the fall and winter. Over time, temporal coverage was improved by developing long-term monitoring systems that could be deployed one season and recovered the next. One of the earliest attempts at this was done in 1967 using five Remote Instrument Packages (creating the unfortunate acronym RIP) installed on the Arctic sea floor for a period of 1 year (Milne and Ganton 1971). When recovered, only 30% of the data was retrieved successfully. The main difficulties were that the data were not available until the retrieval of the system and the actual process of retrieval. Certain systems were even never retrieved due to ice conditions or recovery system failures. Furthermore, since the electronics were exposed to freezing temperatures, they may be prone to breaking and corrupting data before the systems could be recovered (Milne and Ganton 1971; Roth 2008).

More recently, Defence Research and Development Canada (DRDC) conducted a series of persistent monitoring experiments using persistent, multi-sensor observation systems with real-time reporting capability under the Northern Watch

program (Heard et al. 2011a; Forand et al. 2008), deployed in Gascoyne Inlet, Devon Island, Nunavut. The difficult conditions in the Arctic initially caused hardware problems (Carruthers 2016) though preliminary results, including ambient noise and transmission loss data, have been reported (Heard et al. 2011b).

The Barrow Strait Real Time Observatory (BSRTO) was installed after a decade plus observation effort near Resolute, Nunavut, using long-term moorings by Fisheries and Oceans Canada (DFO) at the Bedford Institute of Oceanography (BIO) (Hamilton and Pittman 2015; Hamilton et al. 2013). The system records and transmits daily water property, ice thickness, currents profiles, and passive acoustic data year round. The observatory consists of an underwater network that communicates using acoustic modems to a main mooring, connected to a shore station (in fact, the Northern Watch camp established by DRDC) via an underwater cable.

To reduce the size of the transferred acoustic data, certain processing is done automatically before transmission, while the raw data is saved on the instrument, which is typically retrieved and serviced annually. To conserve battery power and to reduce data transmission bandwidth, the hydrophone is duty-cycled, recording for 1 min every 2 h. BSRTO has been reporting ambient noise data in near real-time over the band 10–800 Hz in 2017–2018 and 10–6400 Hz in 2018–2019. Measurements in 2017 often hit the hydrophone's noise floor of 57 dB ref 1 μPa; thus, a sensor with a higher sensitivity was deployed in September 2018. Figure 6.2 provides a spectrogram of ambient noise measured over fall and winter at BSRTO.
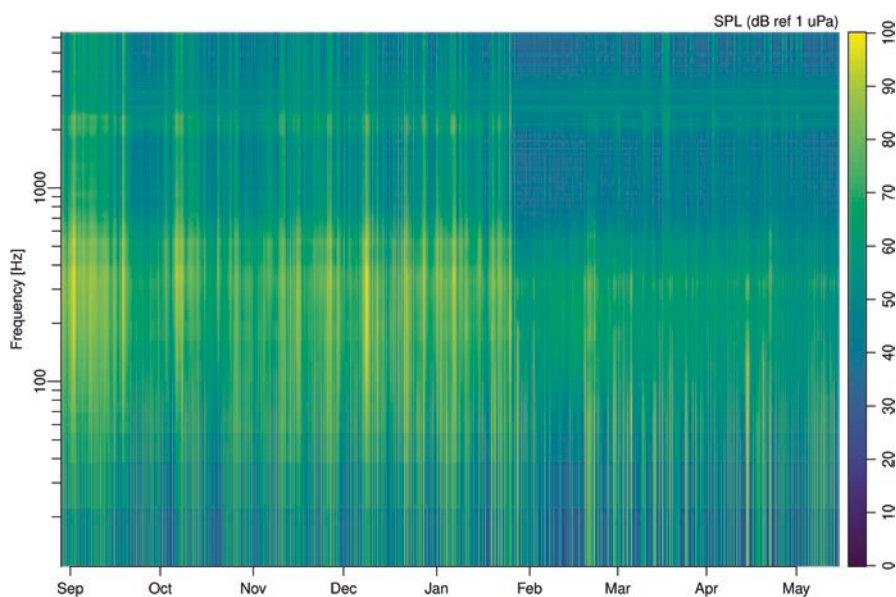


**Fig. 6.2** Spectrogram of data collected at BSRTO between August 2018 and May 2019

### 6.2.2   Spatial Distribution of Measurements

To help distinguish the sources of noise that might contribute to the ambient noise, the Arctic Ocean can be divided into four different regimes (Carey and Evans 2011):

1. The central Arctic: permanently covered with pack ice
2. The coastal regions: covered in shore-fast ice in the winter and a mixture of pack ice and/or ice-free periods during the summer
3. The marginal ice zone: progression from a pack ice region to an ice floe region
4. Open waters: ice-free regions adjacent to the marginal ice zone

In this chapter, data has been divided into three geographical regions. These three regions were chosen to reflect the different regimes as well as to isolate the major study regions in the Canadian Arctic. Zone 1 in Fig. 6.3 is the region with the most ambient noise spectra. It represents the regions north of Alaska and the Yukon known as the Beaufort Sea, consisting of the deep Canadian Basin and wide Chukchi and Beaufort Shelves. The ice conditions vary with season, with the Beaufort Gyre driving first-year and multi-year ice in a clockwise direction. Zone 2 represents the Canadian Archipelago, characterized as a coastal region with seasonal shore-fast ice and shallow water. Finally, Zone 3 represents the central Arctic region, defined by
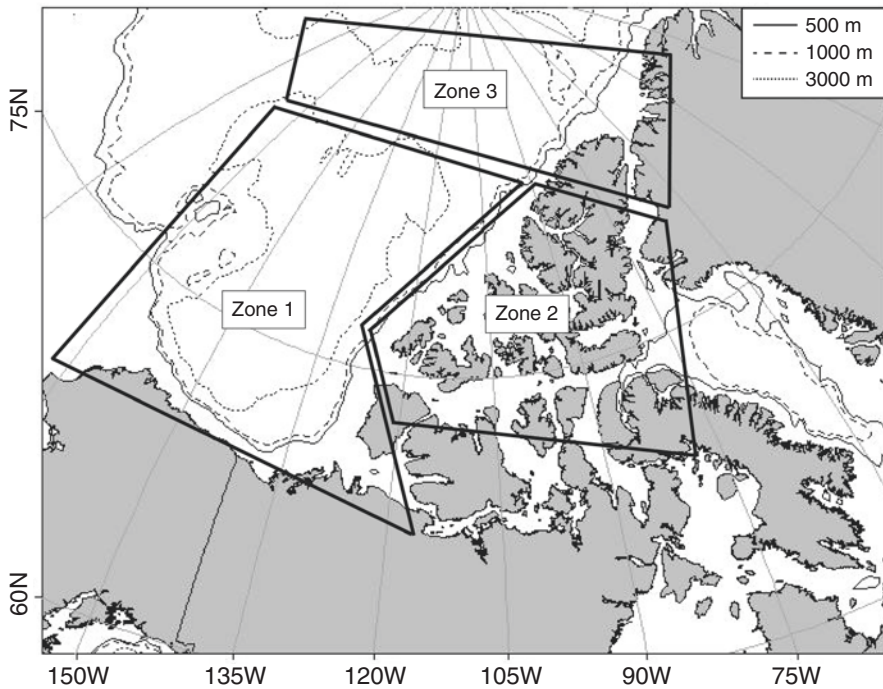


**Fig. 6.3** Map defining different zones of collected data in Figs. 6.4, 6.5, 6.6, and 6.9

persistent multi-year ice. Regions for which no ambient noise spectra were found are the southern region of the Canadian Archipelago[1] and Baffin Bay. Table 6.1 shows the distribution of studies and the different equipment configurations used for the measurements presented in this chapter.

### 6.2.3   Notes on Measurement Quality and Compatibility

Ambient noise levels during quiet periods (e.g., sea state 0 in the open ocean), especially in the low-frequency bands, can be masked by electronic and mechanical system noise or fall below the sensitivity of the sensor (Milne and Ganton 1964; Insley et al. 2017). This can clearly be seen as very narrow band spikes in some spectra under Zone 1 of Fig. 6.4. The spectrum attributed to Chen et al. that has much higher values than the others in Fig. 6.4 was taken during an experiment in the Beaufort Sea in 1994. The study attributed these high-spectrum values to possible high array self-noise during the SIMI94 experiment (Chen et al. 2018).

Most early studies consider ambient noise in the Arctic to be analogous to ocean noise recorded in other basins, free of deterministic transient sources and with quasi-stationary statistics over an appropriate time window, typically greater than 1 min and less, than time scales associated with the changing environmental forcings. Once ice signatures such as thermal cracking were distinguished and identified, certain studies started removing these signals based off the NRC (2003) definition of ambient as noise originating from many indistinguishable sources. Kinda et al. (2013) used a statistical method to isolate and remove ice-generated transients to separate purely ocean-driven noise from ambient noise. Roth et al. (2012) removed transient events from their 2006 data but left them in their 2008–2009 measurements. It would be beneficial for the community to accept a definition of what transient events should be excluded from ambient noise measurements to make noise levels more comparable. The highest peak at 10 Hz in Zone 3 of Fig. 6.6 is due to transients unrelated to the environment, that is, airgun pulses occurring in the surrounding area (Ozanich et al. 2017).

Another factor that makes study inter-comparison difficult is the ambiguity of the units, particularly when considering third octave bands. Here, all measurements are presented as mean-square sound pressure spectral density in dB re 1 $\mu Pa^2$, which is also known as power spectral density (PSD). All values converted to third octave band measurements were assumed, unless otherwise stated, to be averaged and not integrated over the bands. All measurements presented in dB re 1 $\mu Pa$ that were not integrated over frequency bands or stated as sound exposure levels were assumed to be equivalent to dB re 1 $\mu Pa^2$/Hz.

---

[1] Measurements in Pond Inlet, Nunavut, were made in 2016 but have not been reported.

**Table 6.1** Source description of experimental set-up for data shown in Figs. 6.4, 6.5, and 6.6

| Source | Location | Frequency band (Hz) | Set-up | Collection dates | Hydrophone depth (m) | Bottom depth (m) | Notes |
|---|---|---|---|---|---|---|---|
| Chen et al. (2018) | Zone 1 | ~ 10–350 | ICEX16 experiment (anchored vertical array) | March 2016 | 54 | – | Pack ice conditions with a thickness of ~ 1 m |
| Chen et al. (2018) | Zone 1 | ~ 10–350 | SIMI94 experiment (anchored vertical array) | Spring of 1994 | 62 | – | Pack ice conditions with a thickness ≥ 2 m |
| Greene and Buck (1964) | Zone 1 | 25–1000 | Measured from a hydrophone under an ice floe | April 1963 | 60.96 | – | Wind speeds ranging between 0 and 15.4 m/s |
| Insley et al. (2017) | Zone 1 | 10–1000 | Anchored hydrophones | May 2015 to July 2016 | 23.5 | 26.5–28.5 | Coastal location, southwest of Banks Island |
| Kinda et al. (2013) | Zone 1 | 0–4100 | AURAL-M2 autonomous underwater recorder attached to a mooring line | 6 November 2005 to 23 June 2006 | 50 | 397 | Marginal ice zone |
| Lewis and Denner (1988b) | Zone 1 | 10, 32, and 1000 | AIDJEX experiment (from station 10 buoy) | February 1976 | – | ~ 1300 | Winter pack ice |
| Mellen and Marsh (1965) | Zone 1 | ~ 10–1000 | Measured with hydrophones at drift stations T3, Arlis 2, and Polar pack 1 | September–October 1961 and May–September 1962 | 60–180 | – | Variable conditions |
| Roth et al. (2012) | Zone 1 | 10–1000 | Measured from autonomous acoustic recorder (HARP) | September 2006 to May 2009 | 235 | ~ 235 | Variable conditions |
| BSRTO | Zone 2 | 0–6390.63 | Measured with an anchored icListen AF hydrophone | September 2018 to present | 159 | 162 | Off the southwest coast of Devon Island |

(continued)

Table 6.1 (continued)

| Source | Location | Frequency band (Hz) | Set-up | Collection dates | Hydrophone depth (m) | Bottom depth (m) | Notes |
|---|---|---|---|---|---|---|---|
| Ganton and Milne (1965) | Zone 2 | ~ 10–10,000 | Three bottom-mounted hydrophones with 106.68 m space between them | February 1964 | ~ 243.84 | 243.84 | Shore-fast pack ice, 95% was old Arctic pack ice and 5% was 1.83 m-thick fresh lead ice |
| Milne and Ganton (1964) | Zone 2 | 20–10,000 | Bottom-mounted hydrophone | September 1961 | ~ 485 | 485 | Nearly 100% ice cover; 70% first year ice; wind below 7.8 m/s and temperatures ranging between −3 and −6 °C (ice pack 2) |
| Milne et al. (1967) | Zone 2 | ~ 16–5000 | Bottom-mounted hydrophone | 2–5 May 1966 | ~ 451 | 451 | Shore-fast ice |
| Milne and Ganton (1971) | Zone 2 | 150–300 | Remote instrument package installed on the sea floor | 10 September 1967 to 10 October 1967 | – | – | Moving ice floes of various sizes; winds below 11 m/s; temperatures ¡ −37 °C |
| Milne (1974) | Zone 2 | 400–20,000 | Hydrophone lowered through ice | April 1972 | 30 | – | Wind speed of 6.7–11.2 m/s and sea ice thickness of 0.03 m with a mean snow layer thickness of 0.1 m |
| Milne (1974) | Zone 3 | 400–20,000 | Hydrophone lowered through ice | April 1972 | 30 | – | Wind speed of 4.5–6.7 m/s and sea ice thickness of 1.37 m with a mean snow layer thickness of 0.04 m |
| Ozanich et al. (2017) | Zone 3 | ~ 1–976.56 | Drifting array of 22 omnidirectional hydrophones | 4 April to 20 September 2013 | 84.1 (for spectrum presented in Figs. 6.4, 6.5, and 6.6) | 2500 to 4700 | Ice concentrations ranged between 0 and 100% |
| Zakarauskas et al. (1991) | Zone 3 | ~ 2–1000 | – | April 1987 | 55 | 500 | Under pack ice in temperatures ranging between − 26.5 and − 32 °C and wind speeds of 1–9 m/s |

**Fig. 6.4** Accumulation of recorded ambient levels in Zone 1 as defined in Fig. 6.3. Details on how the spectra were collected can be found in Table 6.1 (Greene and Buck 1964; Mellen and Marsh 1965; Lewis and Denner 1988a; Roth et al. 2012; Kinda et al. 2013; Insley et al. 2017; Chen et al. 2018)



**Fig. 6.5** Accumulation of recorded ambient levels in Zone 2 as defined in Fig. 6.3. Details on how the spectra were collected can be found in Table 6.1 (Milne and Ganton 1964, 1971; Ganton and Milne 1965; Milne et al. 1967; Milne 1974)
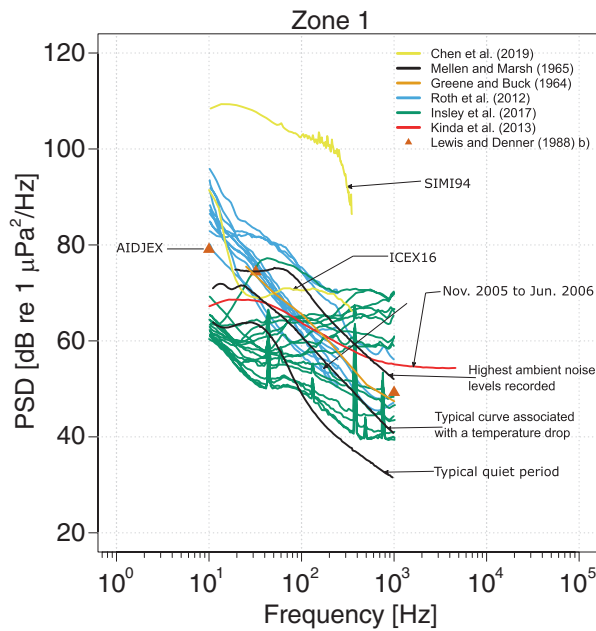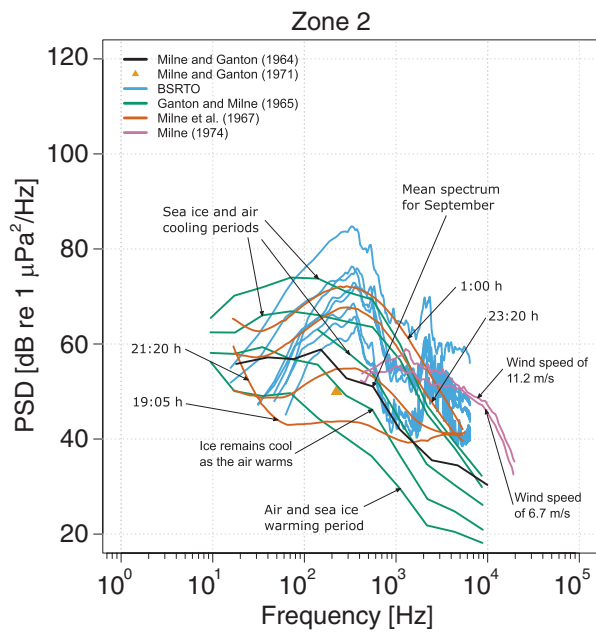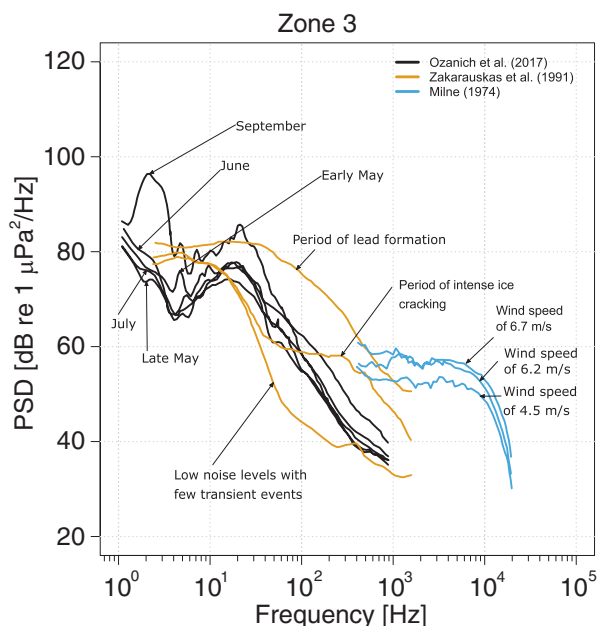
**Fig. 6.6** Accumulation of recorded ambient levels in Zone 3 as defined in Fig. 6.3. Details on how the spectra were collected can be found in Table 6.1 (Milne 1974; Zakarauskas et al. 1991; Ozanich et al. 2017)

## 6.3 Environmental Sources of Noise

### 6.3.1 Ice

Sea ice cover in the Arctic Ocean produces a unique set of sounds related to various mechanical processes within the ice. The characteristics of ice (brittleness, thickness, surface roughness, ridging, and snow cover) along with the outside forces (wind stress, ocean currents, and tidal heave) and the thermodynamic forcing (air temperature) that act on it add new sources to the underwater environment that make predicting and understanding ambient noise in the Arctic more complex than in ice-free oceans, where wave height (or by proxy, wind speed) provides a stable estimate of noise levels (Knudsen et al. 1948; Barclay and Buckingham 2013a). Ice generates noise near the surface boundary under the influence of meteorological conditions, and the mechanisms will change depending on the season and ice cover type (Milne et al. 1967). During shore-fast ice conditions, surface cracks due to thermal gradients will dominate the soundscape. In floe pack ice, relative motion of the flows dominates the soundscape (Milne and Ganton 1964).

Generally, ice cover will skew noise level distributions to low frequencies, as higher frequencies are more readily scattered and absorbed by the ice canopy (Hutt 2012). Spectra dominated by ice noise also have a typical slope of −12 dB per

octave although this can vary drastically depending on the dominant source mechanism (Yang et al. 1987). Low-frequency ice noise is generated by large-scale ice motion ridging, and higher-frequency (kHz − 10's of kHz) noise is induced by particles impinging on the ice surface (Milne 1974) and bubbles bursting as the ice melts (Urick 1971; Hutt 2012).

#### 6.3.1.1 Ice Cracking

Noise from the cracking of ice is usually thermally generated and is an effect observed in pack ice, shore-fast ice, and winter ice. As the air cools, the surface of the ice contracts and cracks; these cracks generate broadband impulsive noise underwater (Ganton and Milne 1965). Ice cracking occurs at the surface where thermal stresses are highest; therefore, these cracks are shallow (0.10–0.15 m deep) (Ganton and Milne 1965; Milne and Ganton 1969, 1971). Cracking is especially prevalent in multi-year ice since it contains less salt and is more brittle (Hutt 2012). As seen in Fig. 6.7, the dashed and dotted lines represent ambient noise levels when cracking is present. A flat spectral shape or a peak near the 100–500 Hz band is the distinguishing feature of a spectrum dominated by thermal ice cracking (Milne and Ganton 1969; Greening and Zakarauskas 1994; Greening et al. 1997; Mellen and Marsh 1965). As air temperature increases, cracking activity will be significantly lower due to the transition of tensile stress to compressive stress (Milne et al. 1967; Milne and Ganton 1969). The resonant frequency of the cracking noise has been hypothesized by Milne and Ganton (1969) to follow Eq. 6.1:

$$f = \left(2\pi d\right)^{-1} \left(\frac{E}{\rho}\right)^{1/2} \left(1+\mu\right)^{-1/2}, \tag{6.1}$$

where f is frequency, E is Young's modulus, d is the crack depth, ρ is the density of the ice, and μ is Poisson's ratio.

#### 6.3.1.2 Ice Ridging

The formation of an ice ridge occurs when two different ice sheets collide, forming a relatively thicker section of ice comprising of a keel on the ocean side and a ridge on the air side. The noise source of this mechanism is from the bottom portion of the keel, which will generate noise at low frequencies and will have a louder sound pressure level (SPL) with thicker ice (Buck and Wilson 1986). According to Greening et al. (1997), spectral peaks centred at around 10 Hz usually represent a noise field dominated by ice-ridging noise. This may be attributed to propagation properties in the Arctic surface channel, which has the lowest attenuation in the band 10–30 Hz (Greening and Zakarauskas 1994; Dyer 1988). Greening and Zakarauskas (1994) demonstrated that source mechanisms with a spectral peak near
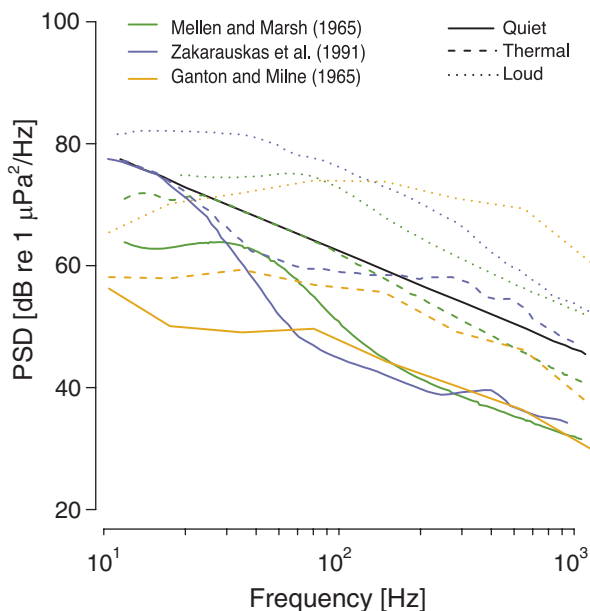
**Fig. 6.7** Arctic ambient noise levels due to cracking using data from Mellen and Marsh (1965), Ganton and Milne (1965), and Zakarauskas et al. (1991) where the solid black line shows a typical ice-free wind-driven noise spectral slope of $-19$ dB/decade or $f^{-5/3}$

10–20 Hz are not required to reproduce observed ambient noise spectra. Broad peaks centred at 10 Hz can be observed in the purple and green curve of the quiet periods in Fig. 6.7 and are due to distant ice ridging.

A model to predict ridge noise was first developed by Pritchard (1984). By assuming that the energy dissipated during the ridging process was a proper measure of the noise source level, Pritchard (1984) was able to explain 46–64% of the noise between 10 and 32 Hz measured in the Beaufort Sea during the AIDJEX project. Another model for ice ridging noise was later developed by Buck and Wilson (1986). They considered the ridge to be a line source and assumed an active ridge spacing of 37 km. They were able to show that the 50 percentile noise levels measured were in good agreement with the model. This shows that ridging noise dominates the average low-frequency ambient noise field in the Arctic. Finally, Pritchard (1990) developed a low-frequency model that used the sum of interactions from ridging, microcracking, and mixed layer shearing to predict ambient noise in the Arctic. The system uses a sea ice dynamic model to predict the distribution and characteristics of the sources. This model generally successfully simulated longer-term trends (daily to weekly) in the CEAREX drift experiment data.

### 6.3.1.3   Other Ice-Related Mechanisms

Diachok and Winokur (1974) studied noise at the ice edge using a horizontal series of sonobuoys. They found that noise levels generated at the ice-water boundary dissipated faster under the ice sheet than in open water and that the difference in dissipation was larger when in the presence of a compact ice versus a diffuse ice edge. They determined that a primary noise-generating mechanism was related to interactions of waves and swells with the ice floes. Yang et al. (1987) determined that the source distribution was not uniform along the ice edge but that noise comes from "hotspots" that act as point sources. The observed distribution of the "hotspots" approximately followed the dimensions and distribution of eddies in the East Greenland Sea (Yang et al. 1987).

Ashokan et al. (2016) studied ice calving and bobbing noises in the Arctic. They observed that an increase in underwater noise under 500 Hz is associated with iceberg calving and bobbing. Tegowskia et al. (2011) also observed a calving event that increased levels at 80 Hz by approximately 17 dB. They compared a location with calving glaciers to a location covered by marine ice floes and found that the site surrounded by calving glaciers had generally lower levels at frequencies below 40 Hz but had levels that were 4–5 dB higher at frequencies above 1000 Hz. The location covered in ice floes had an increase in spectral slop above 5 kHz that was attributed to gas bubbles being released during ice floe collisions, disintegration, and melting (Tegowskia et al. 2011). So far, the overall contribution of calving and bobbing to the Arctic soundscape is unclear (Ashokan et al. 2016).

Ice noise is generally impulsive and can be categorized as a transient signal. A transient signal is short bursts of energy that deviates from a steady state. Kinda et al. (2015) studied local transient signals and divided them into three categories, broadband transients, frequency-modulated tones, and high-frequency broadbands, with centre frequencies ≥1000 Hz. Broadband transients are low-frequency signals that can range between seconds and several minutes (0.9 s and 7 min). Seventy-five percent of the time, their frequency peaks are below 50 Hz and the received levels average at 104 dB re 1 μPa. Kinda et al. (2015) associated these signals with the two first phases of the ice fracturing process. Frequency-modulated tones are signals that cover an even larger bandwidth than broadband transients and have several harmonics. They can repeat at regular intervals and have an average duration that ranges between 1 s and 420 s. These signals have frequencies between 500 Hz and 4 kHz and average receive levels of 95 dB re 1 μPa. Kinda et al. (2015) associated frequency-modulated tones with the reopening of a large lead. Xie and Farmer (1991) and Ye (1995) had observed similar signals, attributing them to friction between newly formed ice flows rubbing longitudinally due to wind and current forcing. High-frequency broadbands can have a continuous or pulsed pattern. They can be distinguished by their long durations and high recorded levels at frequencies above 1 kHz. Their levels have a narrow distribution with a mean of 92 dB re 1 μPa. Kinda et al. (2015) associated these signals with wind effects on frazil ice and did not see a significant link with any kind of precipitation.

### 6.3.2   Wind

Wind will typically generate underwater noise by producing a rough sea state. As the wind speed increases and sea state becomes rougher, the generated underwater noise will increase (Wenz 1962; Urick 1984). This also occurs in the Arctic, but with ice cover, wind will generate noise by crashing ice floes together and by blowing snow and ice over the ice sheets that cover the water. The relationship between wind and noise will change with ice cover and might even be indistinguishable depending on the state of the ice. As opposed to ice-generated noise, wind-generated noise has a Gaussian distribution. Consequently, it can be easily separated from ice ridging and cracking noise using the coefficient of excess. Ganton and Milne (1965) calculated coefficients of excess up to 100 in samples where ice cracking noise dominated. For regions with shore-fast ice cover, Ganton and Milne (1965) were able to identify wind saltation noise (Milne 1974), where ice and snow particles move along the topside of the ice canopy creating high-frequency noise in the water column. Ganton and Milne (1965) derived an empirical equation that related noise levels with wind speed to the power of 5.3. The onset of the relationship occurred at wind speeds between 1.3 and 2.2 *m/s.* Later, Milne (1974) concluded that noise increased with wind speed cubed using data from Ganton and Milne (1965) and Milne et al. (1967).

Milne (1974) also determined a method to calculate wind threshold speed using a model developed by Bagnold (1941) which depends on height, acceleration due to gravity, minimum grain diameter, grain density, density of air, and the aerodynamic roughness. Using data from the Robertson Channel, the theoretical threshold wind speed of 4.1 m corresponded closely to their observations. Milne (1974) also concluded that the shape of the spectrum tends to remain constant once saltation starts.

Milne and Ganton (1971) showed that moving ice flow noise was best correlated with a mean daily wind. In this case, noise was generated by breaking waves and the collision of ice floes. SPL increases with wind speed, and the effects of wind speed are less distinguishable as ice cover concentration and thickness increase (Insley et al. 2017). The relationships of wind speed to noise can be seen in Table 6.2. For Roth et al. (2012), correlations of ambient noise and wind were done for a wind with zero temporal lag.

### 6.3.3   Biological

Most of the detected biological signals are from the western Canadian Arctic and are from bowhead whales, walruses, bearded seals, beluga whales, and grey whales. All of these live year round in the Arctic, except for the grey whale which visits seasonally (Baumgartner et al. 2014). These mammals rely on sound to sense their underwater environments (communication, echolocation, and predator avoidance) (Moore et al. 2012). Bowhead whales make tonal frequency-modulated sounds in the 50–400 Hz range. Beluga whales create whistles, pulsed tones, and noisy

**Table 6.2** Slopes of linear regressions between wind and ambient noise levels at different ice concentrations

| Source | Wind effect coefficient (dB re 1 µPa)/(km/h) | Frequency Hz | Ice cover concentration |
|---|---|---|---|
| Insley et al. (2017) | 0.43 | 250 | Varying ice cover from dates ranging between May 2015 and July 2016 |
| Insley et al. (2017) | 0.14 | 250 | 100% |
| Roth et al. (2012) | 0.28 | 250 | 0–25% |
| Roth et al. (2012) | 0.14 | 250 | 75–100% |
| Milne and Ganton (1971) | 0.6 | 150–300 | Concentration not specified; moving ice floes observed |

vocalizations between 0.4 and 20 kHz. Bearded seal songs will predominantly be in the 1–2 kHz band but may range between 0.02 and 6 kHz. Walruses will mostly produce clicks, rasps, a bell-like tone, and grunts between 0.4 and 1.2 kHz, and grey whales produce knocks and pulses in the 0.1–2 kHz range (Richardson et al. 1995).

All the animals listed have been detected in ambient noise recordings in the Canadian Arctic (Mellen and Marsh 1965; Richardson et al. 1995; Baumgartner et al. 2014). In fact, Clark et al. (2015) showed that, during spring, the chorus of bearded seals dominated the ambient noise levels in the 0.25–2.5 kHz frequency band between the Chukchi and Beaufort Seas. MacIntyre et al. (2013) recorded bearded seals year round and found that their calls coincided with the seasonal ice changes for two consecutive years. Calls increased in the winter with formation of pack ice and peaked in the spring for mating season and preceding the break-up of sea ice.

## 6.4 Anthropogenic Sources of Noise and Their Effect on Marine Mammals

Anthropogenic sources include transportation, dredging, construction, hydrocarbon and mineral exploration and exploitation, geophysical surveys, sonar, explosions, and ocean science studies. In the Arctic, common offshore sources include airgun surveys, pile driving, shipping, ice breaking, dredging, and small boat operations (Moore et al. 2012). Of these, the most widespread source comes from transportation (Giesbrecht 2018). Anthropogenic sources can affect marine mammals by masking important sounds, causing temporary or permanent hearing loss, cause physiological stress or physical injury, and reduce prey availability by causing changes in the ecosystem (Moore et al. 2012). To date, ship noise and airgun noise were of most concern in the Canadian Arctic, and findings have been described in the sections below. A list of studies that focus on the effects of anthropogenic sound on marine maps can be found in Moore et al. (2012), and a review of documented disturbance reactions can be found in Richardson et al. (1995).

### 6.4.1   Ships and Boats

Over the past 20 years, shipping traffic has tripled (Giesbrecht 2018), and with the receding ice cover, existing shipping routes are open longer while new shipping paths could be accessible by the mid-century. In fact, the shorter winter seasons are reducing access to winter roads and making increased boating traffic an even more likely prospect (Stephenson et al. 2011). With increased ship and boat traffic come increased noise and the potential for an increase in disturbance reactions (Moore et al. 2012; Richardson et al. 1995). Shipping traffic generally increases noise levels in the 10–1000 Hz range, which directly overlaps with the calling frequencies of bowhead whales, bearded seals, and ringed seals and could therefore mask their communications (Insley et al. 2017). Furthermore, predictions from the western Canadian Arctic show that loud vessels are audible underwater when they are within 100 km and could affect marine mammal behaviour when within 52 km depending on the vessel type (Halliday et al. 2017). A Monte Carlo simulation study driven by historical observations showed that when a vessel was within the study region, the Tallurutiup Imanga National Marine Conservation Area (TINMCA), the 24-h sound exposure level predicted that vessel noise would be audible to narwhals, belugas, and bowheads for 85%, 81%, and 88% of the time, respectively, but never above the National Oceanic and Atmospheric Administration's limit of temporary threshold shift, where temporary hearing loss will occur (NMFS 2018).

### 6.4.2   Airguns

Airgun pulses are generated by low frequency-controlled sources designed for sub-bottom imaging. Roth et al. (2012) and Ozanich et al. (2017), studies which were conducted in the western and eastern Canadian Arctic, respectively, measured increased SPL in between frequencies of 10 and 30 Hz. Roth et al. (2012) estimated that ambient noise levels in September and October were raised between 2 and 8 dB re 1 µP a2/Hz due to airgun pulses.

## 6.5   Characteristics of Variation

Arctic ambient noise is highly variable and impulsive due its major noise source and major contributor to transmission loss and wave suppression: ice. The wide ranges of ambient noise in the Arctic have been measured to be about 20 dB lower than sea state 0 and up to levels similar to the Knudsen sea state 4 (Urick 1984; Carey and Evans 2011). Ice cracking, ridging, melting, and bobbing will take turns dominating the ambient noise profile depending on the season or study region. Figure 6.8 shows how ice cover type and seasons affect ambient noise levels, based on Hutt's summary of observations from Canadian ice camps and from the BSRTO.

## *6.5.1   Temporal Variations*

### 6.5.1.1   Short Time Scales

The most studied short time variations are due to thermal ice cracking. As the air cools at night, the ice sheet contracts and becomes more brittle making it more susceptible to cracking under tensile stress (Milne and Ganton 1969). This diurnal variation was also observed to be significantly reduced in the presence of snow cover. The snow acts as insulation and slows down the cooling of the ice with the atmospheric temperature (Hutt 2012).

### 6.5.1.2   Long Time Scales

Studies have shown that ambient noise variation does not necessarily follow seasons but is better correlated with month and ice cover type. Arctic seasons can be divided as done by Clark et al. (2015): summer to fall (August to November), spring to summer (April to July), and winter (December to March). In Insley et al. (2017), January to April had the lowest recorded levels, and sound pressure levels were highest between May and October. These trends are also reflected in Fig. 6.8.
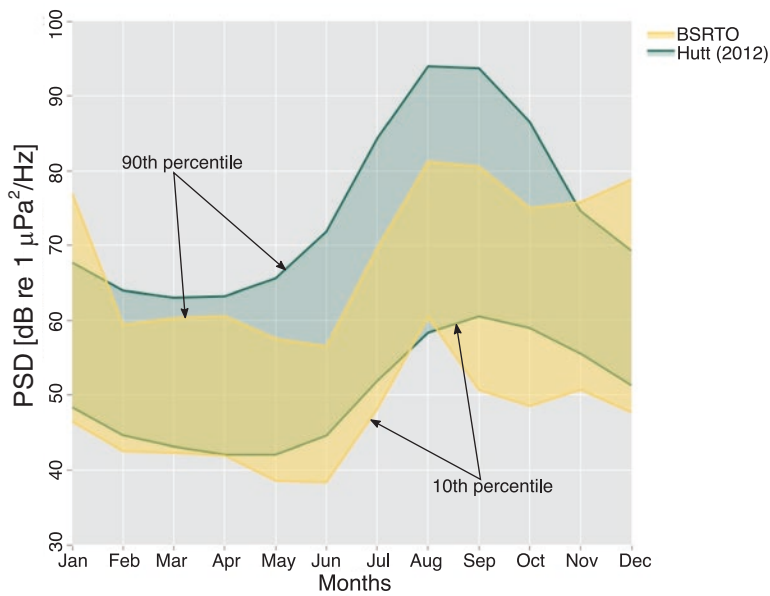


**Fig. 6.8**  Distribution of underwater ambient levels in the Arctic as a function of time of a calendar year for the 10–1000 Hz band, where the shaded region indicates the noise level between the 10th and 90th percentile, as computed by Hutt (2012) (green) and from observations from the BSRTO (yellow)

As seen in Fig. 6.8, July to October shows higher ambient levels due to open water and moving ice flows, which can create high noise levels through collisions. Between December and May, most of the Arctic is covered with pack ice and shore-fast ice, which, although this ice is a source of noise, has quieter ambient noise levels. This is due to increased transmission loss, reduction in biological and anthropogenic sources, and reduction of wind-generated waves by the ice cover. The BSRTO data follows the lower range values presented by Hutt (2012), while the highest values from both curves are recorded between August and September. In December, the noise level at BSRTO increases and widens, which is not seen in Hutt (2012). This difference could be attributed to the BSRTO's single year and sole location of data collection, while the data from Hutt (2012) is an accumulation of data collected at different sites, during various years. Local effects, such as the limited fetch in Barrow Strait and regular weather patterns (e.g., wind direction, ice conditions, freeze-up date), will define the observation, whereas the Hutt data will tend to smooth these effects.

These seasonal trends can also be observed in Fig. 6.9, especially after the 2000s when there were more permanent monitoring systems. Over the frequency band of 150–300 Hz, the PSD will be higher between August and December (blue shades) than January and May (red shades). The levels are also typically highest in August to September and will be lowest in March to May.
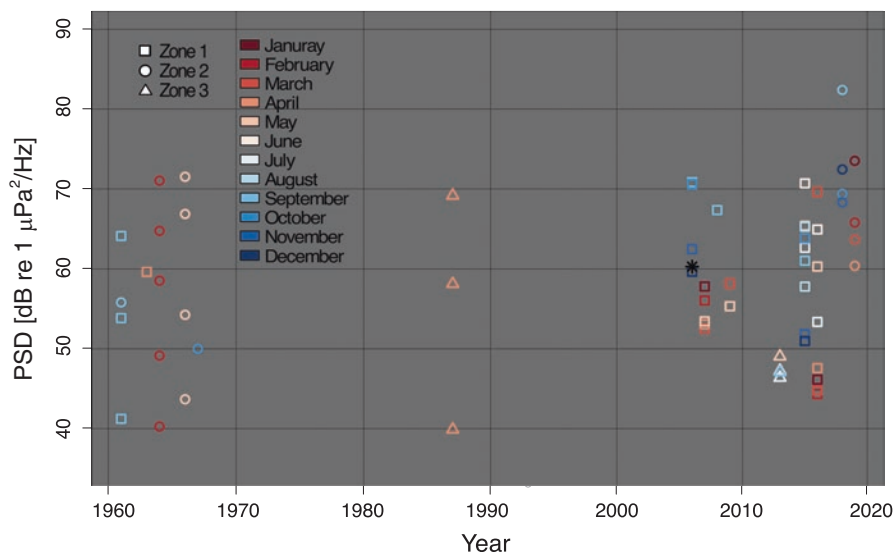


**Fig. 6.9** PSD for the 150–300 Hz band as a function of year collected using the same data as in Figs. 6.4, 6.5, and 6.6. Shapes represent the location of the measurement and colours represent months. If data was collected over 2 months, then the first one was chosen to represent the data. The black star represents data from a year-long mean spectrum taken by Kinda et al. (2013) (Ozanich et al. 2017; Lewis and Denner 1988a, b; Milne and Ganton 1964, 1971; Chen et al. 2018; Zakarauskas et al. 1991; Mellen and Marsh 1965; Ganton and Milne 1965; Greene and Buck 1964; Insley et al. 2017; Roth et al. 2012)

During winter and spring, noise distributions are typically non-Gaussian due to the noise created by the ice, whether it is by cracking, forced collisions due to wind, or other mechanisms. If there are enough events over time and they are distributed evenly enough in space, relative to the recorder, the distribution will be Gaussian (Milne 1966; Zakarauskas et al. 1991; Kinda et al. 2013).

### 6.5.2   Spatial Variations

As seen in Figs. 6.4, 6.5, and 6.6, the PSD levels in each zone cover a wide range of values. All the measurements were made over the 10–1000 Hz band and have similar slopes. Two exceptions occur: a single spectrum in Zone 1 shown in Fig. 6.4. and those made by Insley et al. (2017), which were collected in very shallow water and are presumably more influenced by local surface ice noise and ice interactions with the bottom. The seminal measurements of Mellen and Marsh (1965) do a remarkable job in summarizing observations succinctly.

Spectra in Zone 2, with the exception of the BSRTO data, were all taken with the purpose of understanding the effect of ice cracking on ambient noise and thus were computed on short time scales. Measurements were taken at different times of day when cracking was known to be quiet or loud due to forcing by atmospheric heating and cooling. BSRTO data, shown as monthly averages, have a peak at 2.5 kHz, corresponding with the horizontal bands shown in Fig. 6.2. The source of this broadband noise may be due to mechanical noise generated by the mooring, though further study is required.

Spectra in Zone 3 have peaks between 10 and 50 Hz. All measurements in Zone 3 were taken at depths shallower than 85 m, which is within the shallow propagation channel created by the sounds speed profile. Distant airgun-generated noise is observable during the open water months, particularly in the September data of Ozanich et al. (2017).

### 6.5.3   Depth Dependence

Though the spatial properties of noise are important for predicting sonar performance, only Greene and Buck (1964) and Ozanich et al. (2017) have reported on the depth dependence of Arctic ambient noise. Greene and Buck (1964) determined that minimum noise intensity is at the bottom of the ice, increasing to a uniform depth dependence beyond a depth of one-half the wave length. Ozanich et al. (2017) replicated those observations using a drifting array and concluded that noise time series tends to become normally distributed as the sensor depth increases and the receiver effectively monitors a larger area of the surface, an effect also seen in the ice-free ocean (Vagle et al. 1990; Barclay and Buckingham 2013b). Close to the ice, local overpowering transients skew the noise signal towards non-Gaussianity.

## 6.6   Propagation

To both develop a model of natural ambient noise and quantify the effect of anthropogenic sources on the underwater soundscape in the Canadian Arctic, accurate knowledge of underwater sound transmission loss is required. Transmission loss in the Arctic is affected by mechanisms related to the ice canopy, as well as scattering and reflection from the seabed and volume scattering and absorption. Considerable experimental and theoretical efforts have been invested into understanding these mechanisms since the middle of the previous century, though an accurate model of a rough, elastic sea ice layer has yet to be demonstrated. The ice layer contributes to transmission loss through scattering from the rough underside layer, comprised of a local surface roughness as well as large keels (ridges), through the conversion of compressional energy to shear energy in the ice layer and interface waves and through the bulk acoustic wave properties within the ice itself, such as compressional and shear attenuation. The wave speed structure and attenuation within the ice layer depends on parameters such as temperature, salinity, and density (Rajan et al. 1993). Sea ice thickness can range from a fraction of a wavelength to multiple wavelengths, making these effects highly frequency dependent.

   Due to the dynamic nature of atmospheric and oceanographic conditions in the Arctic, the material properties within the sea ice undergo significant seasonal changes and are subject to large spatial variability. Additionally, the measurement of the ocean ice roughness profile and the acoustic properties within the ice layer over long ranges is technically and logistically challenging. As a result, simplified analytical models and statistical methods are typically employed for predicting transmission loss in the Arctic. A range of propagation models have been developed, including empirically derived relationships, ray models, normal mode models, wave number integral models, and parabolic equation (PE) models of varying complexity. This section provides a brief overview of under-ice transmission loss measurements and modelling.

### 6.6.1   Measurements

Figure 6.1 shows that in both summer and winter, the upward refracting environment in the Arctic allows for very long-range transmission of sound that is either surface trapped or in a shallow sound channel centred at 150 m depth. In the ice-free ocean, the air-sea interface is perfectly reflecting, making a surface trapped waveguide an efficient propagation channel. Surface roughness due to wind waves and swell, and bubble layers due to breaking waves, can reduce the channels' efficiency through scattering and cause a deterministic signal to lose coherence as it repeatedly interacts with the surface.

   Similarly, the underside of the sea ice layer adds losses due to scattering and reflection, phenomena quantified in early measurement by Buck and Greene (1964)

who measured aircraft-deployed explosive sources at ranges of up to 200 km in the deep Arctic Ocean. The frequency-dependent effective attenuation of the ice layer was observed to begin at 50 Hz and increase with frequency (Fig. 6.10). During the same period, Marsh and Mellen (1963) conducted transmission loss experiments over a distance of 800 km and similarly demonstrated the strong frequency dependence caused by the ice layer.

At the time, Canadian defence researchers began studying sound propagation in Barrow Strait, a shallow water environment where both the ice layer and the seabed contribute to transmission loss. Milne (1960) observed a loss consistent with geometric spreading, in this case cylindrical, over a relatively short range of 18 km with an added 1 dB of loss in the 10–20 kHz band per 1.8 km (nautical mile) (Fig. 6.10). At these ranges, Milne noted that transmission times between fixed stations were more stable than in the open ocean (Ganton et al. 1969).

In order to estimate the importance of ice keels on transmission loss, observations of ice ridge densities and sail height were used to infer keel number densities and draft in the central Arctic (Zones 1 and 3) by Diachok (1976) and used as input parameters for a propagation model that treats the ice as a pressure release (perfect) scatterer. The results were used to estimate a frequency-dependent effective attenuation in two different regions of the Arctic, as shown in Fig. 6.10. During this time, a Canadian effort by Verrall and Ganton (1977) was focused on improving estimates
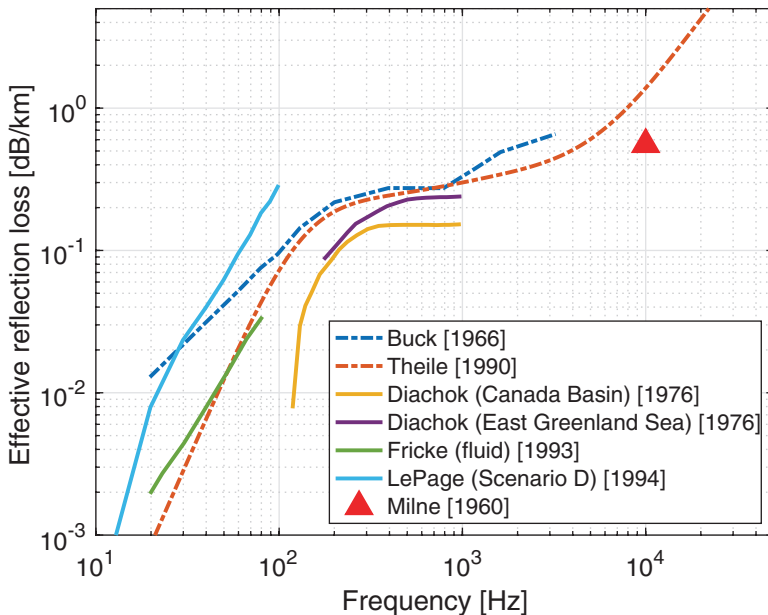


**Fig. 6.10** Effective attenuation per unit distance due to ice cover as a function of frequency according to observations (solid red triangle) (Milne 1960), empirical relationships (dashed lines) derived by Buck and Greene (1964) and Thiele et al. (1990), and physics-based models by Diachok (1976), Fricke (1993), and LePage and Schmidt (1994)

of the reflection coefficient of shore-fast ice in the Canadian Archipelago. Further experiments were carried out to improve the sea ice reflection coefficient at low frequency (Livingston and Diachok 1989), and theoretical progress was made on rough ice scattering models (Kuperman and Schmidt 1986).

The next series of measurements began in the early 1990s and were planned as basin-scale tomographic experiments. By sending precisely timed tomographic signals across the Arctic basin, the travel times along various deep diving, shallow diving, and surface interacting acoustic paths can be used to compute the sound speed (thus temperature and salinity) in depth and range, as well as the ice thickness and roughness. The Transarctic Acoustic Propagation (TAP) experiment was planned as a demonstration project to measure the warming of the Arctic Ocean basin between a source placed north of Spitzbergen and two receivers, one near Barrow, Alaska, and a second near Alert, Nunavut (Mikhalevsky et al. 1995, 1999). The 6-day experiment successfully detected the intrusion of warm Atlantic Intermediate Water using a 20.5 Hz signal and led to improved scattering models for the ice-water interface (LePage and Schmidt 1994; Fricke 1993) (Fig. 6.10). This sets the stage for a year-long monitoring program, Arctic Climate Observations Using Underwater Sound (ACOUS), deployed in 1998. ACOUS used a similar geometry and source to TAP and successfully inferred the seasonal ice thickness and roughness, using a scattering inverse model by Kudryashov (1996) (Gavrilov and Mikhalevsky 2006).

Tomographic measurements in the Arctic have continued to the present day, with persistent monitoring and increasingly complex ocean acoustic-coupled models. A series of experiments monitored the Fram Strait during the previous decade (Sagen et al. 2016) resulting in studies of small- to large-scale processes (e.g., internal waves to global scale currents) (Dushaw et al. 2016a, b). In the Canadian Arctic, the Canada Basin Acoustic Propagation Experiment (CANAPE) recently concluded, with early results demonstrating the effect of the Beaufort Gyre throughout the year on propagation between the central Arctic and the Chukchi Shelf (Worcester 2015; Ballard et al. 2017). Analysis from these recent data sets will push the underwater acoustics community to advance low-frequency, under-ice propagation models (Collins et al. 2019), ocean acoustic-coupled models (Duda et al. 2018; Ballard et al. 2017), and three-dimensional propagation models. These advances will better allow the modelling of anthropogenic activity, namely, shipping and oil and gas exploration, in the Canadian Arctic.

### 6.6.2   Modelling

Buck (1966) used their early measurements of under-ice transmission loss to develop an empirical model that combines geometric spreading with a frequency-dependent effective reflection loss per unit distance term (Fig. 6.10). The model was fit to the data at nine frequencies in the band 20–3200 Hz, where the standard deviation for each fit ranged between ±5 and ± 9 dB. Empirically derived models, such as

the more recent Thiele et al. (1990) equation, and data summaries, such as the one provided in Urick (1984), provide rapid estimates of transmission loss but fail to account for the spatial diversity in ice layer properties, as well as the seasonal and climate change-driven temporal variability. For this reason, a portable, physics-based model of under-ice propagation is desirable.

The early efforts of Marsh and Mellen (1963) and Milne (1960) both focused on ray models for quantifying the loss due to ice and worked on estimating reflection loss coefficients for the ice-water interface. Diachok (1976) continued this effort, incorporating scattering from semi-cylindrical ice ridges (keels) into a ray tracing model. The majority of modelling development was then directed at better scattering physics, ice-water reflection coefficients, and the incorporation of keels and roughness into ray tracing and normal mode models (Kuperman and Schmidt 1989; Fricke 1993; LePage and Schmidt 1994; Kudryashov 1996).

Kuperman and Schmidt (1986) implemented a full-wave solution to a horizontally stratified ocean waveguide with a random rough interface between any combination of fluid and elastic layers. This model was able to account for scattering at the ice-water interface and the conversion of compressional energy to shear energy, but only for range-independent problems. This model has provided accurate predictions of arrival times for recent tomography measurements in the Fram Strait (Hope et al. 2017).

Gavrilov and Mikhalevsky (2006) used a normal mode propagation code to demonstrate that the ACOUS tomographic signals likely contained information on the ice thickness, though the range-dependent environment added uncertainty to the result. In another study, a finite-difference numerical simulation showed both the elastic parameters and a rough interface have frequency-dependent effects on the propagated and scattered fields, though it was the simulation of fluid ice keels that best fits the observations (Fricke 1993).

In the preceding decades, PE propagation models had grown in capability, reliability, and accuracy and offered the advantage of accommodating range-dependent environments at low frequencies, where ray models tended to have difficulty computing transmission loss. Recent advances allowed a fully elastic seabed and ice canopy to be incorporated into a PE simulation (Collins 2012, 2015). Collis et al. (2016) benchmarked such a model against an elastic normal mode code and wave number integration solution and demonstrated the PE model's ability to compute transmission loss under a slowly varying range-dependent ice thickness. Collins et al. (2019) was further able to demonstrate scattering from a data-derived ice surface with keels using a fully elastic PE code over a model range of 40 km.

Diachok (1976) showed that a pressure release rough surface could do a good job of matching data, provided the statistics of the keels were well known. When scattering is the dominant loss mechanism, the same approximation may be applied to a range-dependent propagation model without the added computational complexity of a thin, elastic interface. Ballard (2019) implemented a three-dimensional hybrid PE-normal mode propagation code with a pressure release rough surface. She found that horizontal reflections from ice keels cause the predicted standard deviation of received levels over the model area, though the mean remained nearly constant.

The recent demonstration of a fully elastic PE code capable of roughness on the length scale of ice keels represents a significant advancement in under-ice sound propagation modelling (Collins et al. 2019). Careful model data comparisons are required to fully quantify the relative loss contributions of scattering due to roughness and ice keels and shear energy conversion. In some cases, range-independent elastic models may suffice, while in others, inelastic pressure release rough ice may capture the dominant physics relevant to predicting transmission loss.

## 6.7   Conclusion

The changing ice conditions in the Canadian Arctic will alter the underwater soundscape through spatial and temporal shifts in the natural noise-generating mechanisms, a reduction in ice-driven transmission loss, and an increase in the presence of industrial activity, including shipping. A review of historical measurements demonstrates that the power spectral density at any given frequency in the 10 Hz to 10 kHz band may vary by 30 dB in the deep water environment of the Beaufort Sea or Canada Basin (Zone 1), between 30 and 40 dB in the shallow Canadian Archipelago (Zone 2), and by 20 dB in the Lincoln Sea (Zone 3), where multi-year ice persists.

These large variations are driven by seasonal variations in forcings, with increased ice-generated noise occurring during freeze-up and break-up, increased wind noise during open water, and periods of quiet arriving with shore-fast ice. Contemporary measurements made by the BSRTO demonstrate this seasonality, shown in Fig. 6.8, which compares well with historical measurements made at locations throughout the Archipelago between 1962 and 1987 (Hutt 2012). In both data summaries, the noisiest time occurs during the open water season (August and September) when sound generated by wind wave dominates, and the quietest season (February to May) is when stable, shore-fast ice is present.

The year-round BSRTO acoustic data, along with concurrent oceanographic, ice draft, and meteorological data, presents a significant opportunity to advance the ability to predict and model natural ambient noise in the Canadian Archipelago and in ice-covered waters in general, using a physics-based and portable approach.

Accurate modelling of the natural noise field is a necessary component of a marine spatial planning tool capable of quantifying the potential noise impact of industrial activity, including shipping, and presenting useful and meaningful information to decision-makers. The other key component of such a tool is a high-fidelity transmission loss model capable of operating in a range-dependent, partially or fully ice-covered environment. Recent advances in under-ice sound propagation modelling appear to meet these requirements, though further validation is required, particularly in shallow water and over long ranges. The combination of a portable Arctic transmission loss model and ambient noise model, along with an understanding of the sensitivity of their accuracy to input data quality (such as per cent ice cover, ice draft, sound speed profile, and meteorological conditions), will allow the

realistic prediction of the acoustic footprint of vessels, airguns, and other industrial sound sources. Once validated, such a tool could provide an accurate representation of the acoustic impact of future use and simulate the effect of management solutions.

# References

Ashokan, M., Latha, G., Thirunavukkarasu, A., Raguruman, G., & Venkatesan, R. (2016). Ice berg cracking events as identified from underwater ambient noise measurements in the shallow waters of Ny-alesund, Arctic. *Polar Science, 10*(2), 140–146.

Bagnold, R. A. (1941). *The physics of blown sand and desert dunes*. Methuen.

Ballard, M. S. (2019). Three-dimensional acoustic propagation effects induced by the sea ice canopy. *The Journal of the Acoustical Society of America, 146*(4), EL364–EL368.

Ballard, M. S., Sagers, J. D., Lin, Y. T., Badiey, M., Worcester, P. F., & Pecknold, S. (2017). Acoustic propagation from the Canadian basin to the Chukchi shelf. *The Journal of the Acoustical Society of America, 142*(4), 2713–2713.

Barclay, D. R., & Buckingham, M. J. (2013a). Depth dependence of wind-driven, broadband ambient noise in the Philippine Sea. *The Journal of the Acoustical Society of America, 133*(1), 62–71.

Barclay, D. R., & Buckingham, M. J. (2013b). The depth-dependence of rain noise in the Philippine Sea. *The Journal of the Acoustical Society of America, 133*(5), 2576–2585.

Baumgartner, M. F., Stafford, K. M., Winsor, P., Statscewich, H., & Fratantoni, D. M. (2014). Glider-based passive acoustic monitoring in the Arctic. *Marine Technology Society Journal, 48*(5), 40–51.

Buck, B. M. (1966). *Arctic acoustic transmission loss and ambient noise*. Santa Barbara: Sea Operations Department, GM Defense Research Labs.

Buck, B. M., & Greene, C. R. (1964). Arctic deep-water propagation measurements. *The Journal of the Acoustical Society of America, 36*(8), 1526–1533.

Buck, B. M., & Wilson, J. H. (1986). Nearfield noise measurements from an Arctic pressure ridge. *The Journal of the Acoustical Society of America, 80*(1), 256–264.

Carey, W. M., & Evans, R. B. (2011). *Ocean ambient noise measurement and theory*. New York: Springer.

Carruthers, W. (2016). *An array of blunders: The Northern Watch Technology Demonstration Project*. Niobe Paper No. 1. Naval Association of Canada.

Chen, R., Poulsen, A., & Schmidt, H. (2018). Spectral, spatial, and temporal characteristics of underwater ambient noise in the Beaufort Sea in 1994 and 2016. *The Journal of the Acoustical Society of America, 144*(3), 1695.

Clark, C. W., Berchok, C. L., Blackwell, S. B., Hannay, D. E., Jones, J., Ponirakis, D., & Stafford, K. M. (2015). A year in the acoustic world of bowhead whales in the Bering, Chukchi and Beaufort seas. *Progress in Oceanography, 136*, 223–240.

Collins, M. D. (2012). A single-scattering correction for the seismo-acoustic parabolic equation. *The Journal of the Acoustical Society of America, 131*(4), 2638–2642.

Collins, M. D. (2015). Treatment of ice cover and other thin elastic layers with the parabolic equation method. *The Journal of the Acoustical Society of America, 137*(3), 1557–1563.

Collins, M. D., Turgut, A., Menis, R., & Schindall, J. A. (2019). Acoustic recordings and modeling under seasonally varying sea ice. *Scientific Reports, 9*(1), 8323.

Collis, J. M., Frank, S. D., Metzler, A. M., & Preston, K. S. (2016). Elastic parabolic equation and normal mode solutions for seismo-acoustic propagation in underwater environments with ice covers. *The Journal of the Acoustical Society of America, 139*(5), 2672–2682.

Diachok, O. I. (1976). Effects of sea-ice ridges on sound propagation in the Arctic Ocean. *The Journal of the Acoustical Society of America, 59*(5), 1110–1120.

Diachok, O. I., & Winokur, R. S. (1974). Spatial variability of underwater ambient noise at the Arctic ice-water boundary. *The Journal of the Acoustical Society of America, 55*(4), 750–753.

Duda, T. F., Lin, Y. T., Zhang, W. G., Colosi, J. A., & Badiey, M. (2018). Arctic Beaufort Gyre duct transmission measurements and simulations. *The Journal of the Acoustical Society of America, 144*(3), 1666.

Dushaw, B. D., Sagen, H., & Beszczynska-Möller, A. (2016a). On the effects of small-scale variability on acoustic propagation in Fram Strait: The tomography forward problem. *The Journal of the Acoustical Society of America, 140*(2), 1286–1299.

Dushaw, B. D., Sagen, H., & Beszczynska-Möller, A. (2016b). Sound speed as a proxy variable to temperature in Fram Strait. *The Journal of the Acoustical Society of America, 140*(1), 622–630.

Dyer, I. (1988). *Sea surface sound*. Kluwer Academic Publishers.

Forand, J. L., Larochelle, V., Brookes, D., Lee, J. P. Y., MacLeod, M., Dao, R., Heard, G. J., McCoy, N., & Kollenberg, K. (2008). *Surveillance of Canada's high Arctic*. IEEE OCEANS 2008 (pp. 1–8), 15–18 September 2008, Quebec City, Canada.

Fricke, R. J. (1993). Acoustic scattering from elemental Arctic ice features: Numerical modeling results. *The Journal of the Acoustical Society of America, 93*(4), 1784–1796.

Ganton, J. H., & Milne, A. R. (1965). Temperature and wind-dependent ambient noise under midwinter pack ice. *The Journal of the Acoustical Society of America, 38*(3), 406–411.

Ganton, J. H., Milne, A. R., & Hughes, T. (1969). *Acoustic stability at long ranges under shore-fast ice*. Technical Report 69–3. Victoria (Canada): Defence Research Establishment Pacific.

Gavrilov, A. N., & Mikhalevsky, P. N. (2006). Low-frequency acoustic propagation loss in the Arctic Ocean: Results of the Arctic climate observations using underwater sound experiment. *The Journal of the Acoustical Society of America, 119*(6), 3694–3706.

Giesbrecht, E. E. (2018). Acoustic modelling to inform policies: Mitigating vessel noise impacts on Arctic cetaceans within the Tallurutiup Imanga National Marine Conservation Area. Master's thesis, Dalhousie University, Halifax, Canada, 2018.

Greene, C. R., & Buck, B. M. (1964). Arctic Ocean ambient noise. *The Journal of the Acoustical Society of America, 36*(6), 1218–1220.

Greening, M. V., & Zakarauskas, P. (1994). Pressure ridging spectrum level and a proposed origin of the 20-Hz peak in Arctic ambient noise spectra. *The Journal of the Acoustical Society of America, 90*(4), 2313.

Greening, M. V., Zakarauskas, P., & Dosso, S. E. (1997). Matched-field localization for multiple sources in an uncertain environment, with application to Arctic ambient noise. *The Journal of the Acoustical Society of America, 101*(6), 3525–3538.

Halliday, W. D., Insley, S. J., de Jong, T., & Pine, M. K. (2017). Potential impacts of shipping noise on marine mammals in the western Canadian Arctic. *Marine Pollution Bulletin, 123*(1–2), 73–82.

Hamilton, J. M., & Pittman, M. D. (2015). Sea-ice freeze-up forecasts with an operational ocean observatory. *Atmosphere-Ocean, 53*(5), 595–601.

Hamilton, J. M., Collins, K., & Prinsenberg, S. J. (2013). Links between ocean properties, ice cover, and plankton dynamics on interannual time scales in the Canadian Arctic archipelago. *Journal of Geophysical Research: Oceans, 118*(10), 5625–5639.

Heard, G. J., Pelavas, N., Lucas, C. E., Peraza, I., Clark, D., Cameron, C., & Shepeta, V. (2011a). Development of low-cost underwater acoustic array systems for the northern watch technology demonstration project. *Canadian Acoustics, 39*(3), 200–201.

Heard, G. J., Pelavas, N., Ebbeson, G. R., Hutt, D. L., Peraza, I., Schattschneider, G., Clark, D., Shepeta, V., & Rouleau, J. (2011b). *Underwater sensor system 2009 field trial report*. Technical memorandum 2010–241. Dartmouth (Canada): Defence Research and Development Canada–Atlantic.

Hope, G., Sagen, H., Storheim, E., Hobæk, H., & Freitag, L. (2017). Measured and modeled acoustic propagation underneath the rough Arctic Sea ice. *The Journal of the Acoustical Society of America, 142*(3), 1619–1633.

Hutt, D. L. (2012). An overview of Arctic Ocean acoustics. *AIP Conference Proceedings, 1495*, 56–58.

Insley, S. J., Halliday, W. D., & de Jong, T. (2017). Seasonal patterns in ocean ambient noise near Sachs harbour, Northwest Territories. *Arctic: Journal of the Arctic Institute of North America, 70*(3), 239–248.

Kinda, G. B., Simard, Y., Gervaise, C., Mars, J. I., & Fortier, L. (2013). Under-ice ambient noise in eastern Beaufort Sea, Canadian Arctic, and its relation to environmental forcing. *The Journal of the Acoustical Society of America, 134*(1), 77–87.

Kinda, G. B., Simard, Y., Gervaise, C., Mars, J. I., & Fortier, L. (2015). Arctic underwater noise transients from sea ice deformation: Characteristics, annual time series, and forcing in Beaufort Sea. *The Journal of the Acoustical Society of America, 138*(4), 2034–2045.

Knudsen, V. O., Alford, R. S., & Emling, J. W. (1948). Underwater ambient noise. *Journal of Marine Research, 7*(3), 410–429.

Kudryashov, V. M. (1996). Sound reflection from ice cover. *Acoustical Physics, 42*(2), 215–221.

Kuperman, W. A., & Schmidt, H. (1986). Rough surface elastic wave scattering in a horizontally stratified ocean. *The Journal of the Acoustical Society of America, 79*(6), 1767–1777.

Kuperman, W. A., & Schmidt, H. (1989). Self-consistent perturbation approach to rough surface scattering in stratified elastic media. *The Journal of the Acoustical Society of America, 86*(4), 1511–1522.

LePage, K., & Schmidt, H. (1994). Modeling of low-frequency transmission loss in the central Arctic. *The Journal of the Acoustical Society of America, 96*(3), 1783–1795.

Lewis, J. K., & Denner, W. W. (1988a). Arctic ambient noise in the Beaufort Sea: Seasonal relationships to sea ice kinematics. *The Journal of the Acoustical Society of America, 83*(2), 549–565.

Lewis, J. K., & Denner, W. W. (1988b). Higher frequency ambient noise in the Arctic Ocean. *The Journal of the Acoustical Society of America, 84*(4), 1444–1455.

Livingston, E., & Diachok, O. I. (1989). Estimation of average under-ice reflection amplitudes and phases using matched-field processing. *The Journal of the Acoustical Society of America, 86*(5), 1909–1919.

MacIntyre, K. Q., Stafford, K. M., Berchok, C. L., & Boveng, P. L. (2013). Year-round acoustic detection of bearded seals (*Erignathus barbatus*) in the Beaufort Sea relative to changing environmental conditions, 2008–2010. *Polar Biology, 36*(8), 1161–1173.

Marsh, H. W., & Mellen, R. H. (1963). Underwater sound propagation in the Arctic Ocean. *The Journal of the Acoustical Society of America, 35*(4), 552–563.

Mellen, R. H., & Marsh, H. W. (1965). *Underwater sound in the Arctic Ocean*. Technical report MED-65-1002. New London, CT: U.S. Navy Underwater Sound Laboratory.

Mikhalevsky, P. N., Baggeroer, A. B., Gavrilov, A., & Slavinsky, M. (1995). Experiment tests use of acoustics to monitor temperature and ice in Arctic Ocean. *Eos, Transactions American Geophysical Union, 76*(27), 265–269.

Mikhalevsky, P. N., Gavrilov, A. N., & Baggeroer, A. B. (1999). The transarctic acoustic propagation experiment and climate monitoring in the Arctic. *IEEE Journal of Oceanic Engineering, 24*(2), 183–201.

Milne, A. R. (1960). Shallow water under-ice acoustics in Barrow Strait. 1960. *The Journal of the Acoustical Society of America, 32*(8), 1007–1016.

Milne, A. R. (1966). Statistical description of noise under shore-fast ice in winter. *The Journal of the Acoustical Society of America, 39*(6), 1174–1182.

Milne, A. R. (1974). Wind noise under winter ice fields. *Journal of Geophysical Research, 79*(6), 803–809.

Milne, A. R., & Ganton, J. H. (1964). Ambient noise under Arctic-sea ice. *The Journal of the Acoustical Society of America, 36*(5), 855–863.

Milne, A. R., & Ganton, J. H. (1969). Diurnal variations in underwater noise beneath springtime sea-ice. *Nature, 221*, 851–852.

Milne, A. R., & Ganton, J. H. (1971). Noise beneath sea ice and its dependence on environmental mechanisms. *U.S. Navy Journal of Underwater Acoustics, 21*(1), 69–81.

Milne, A. R., Ganton, J. H., & McMillan, D. J. (1967). Ambient noise under sea ice and further measurements of wind and temperature dependence. *The Journal of the Acoustical Society of America, 41*(2), 525–528.

Moore, S. E., Reeves, R. R., Southall, B. L., Ragen, T. J., Suydam, R. S., & Clark, C. W. (2012). A new framework for assessing the effects of anthropogenic sound on marine mammals in a rapidly changing Arctic. *Bioscience, 62*(3), 289–295.

NMFS (National Marine Fisheries Service). (2018). *2018 revision to: Technical guidance for assessing the effects of anthropogenic sound on marine mammal hearing (version 2.0): Underwater thresholds for onset of permanent and temporary threshold shifts*. NOAA technical memorandum NMFS-OPR-59. Silver Spring, MD: National Oceanic and Atmospheric Administration, U.S. Department of Commerce.

NRC (National Research Council). (2003). *Ocean noise and marine mammals*. Washington, DC: The National Academies Press.

Ozanich, E., Gerstoft, P., Worcester, P. F., Dzieciuch, M. A., & Thode, A. (2017). Eastern Arctic ambient noise on a drifting vertical array. *The Journal of the Acoustical Society of America, 142*(4), 1997–2006.

Pritchard, R. S. (1984). Arctic Ocean background noise caused by ridging of sea ice. *The Journal of the Acoustical Society of America, 75*(2), 419–427.

Pritchard, R. S. (1990). Sea ice noise-generating processes. *The Journal of the Acoustical Society of America, 88*(6), 2830–2842.

Rajan, S. D., Frisk, G. V., Doutt, J. A., & Sellers, C. J. (1993). Determination of compressional wave and shear wave speed profiles in sea ice by crosshole tomography: Theory and experiment. *The Journal of the Acoustical Society of America, 93*(2), 721–738.

Richardson, W. J., Greene, C. R., Jr., Malme, C. I., & Thomson, D. H. (1995). *Marine mammals and noise*. San Diego: Academic Press.

Roth, E. H. (2008). Arctic Ocean long-term acoustic monitoring: Ambient noise, environmental correlates and transients north of Barrow, Alaska. Master's thesis, University of California, San Diego, California.

Roth, E. H., Hildebrand, J. A., Wiggins, S. M., & Ross, D. (2012). Underwater ambient noise on the Chukchi Sea continental slope from 2006–2009. *The Journal of the Acoustical Society of America, 131*(1), 104–110.

Sagen, H., Dushaw, B. D., Skarsoulis, E. K., Dumont, D., Dzieciuch, M. A., & Beszczynska-Möller, A. (2016). Time series of temperature in Fram Strait determined from the 2008–2009 DAMOCLES acoustic tomography measurements and an ocean model. *Journal of Geophysical Research: Oceans, 121*(7), 4601–4617.

Stephenson, S. R., Smith, L. C., & Agnew, J. A. (2011). Divergent long-term trajectories of human access to the Arctic. *Nature Climate Change, 1*, 156–160.

Tegowskia, J., Deane, G. B., Lisimenka, A., & Blondel, P. (2011). Detecting and analyzing underwater ambient noise of glaciers on Svalbard as indicator of dynamic processes in the Arctic. *Proceedings of the Institute of Acoustics, 33*, 83–85.

Thiele, L., Larsen, A., & Nielsen, O. W. (1990). *Underwater noise exposure from shipping in Baffin Bay and Davis Strait*. Report 87.184. Copenhagen: Ødegaard & Danneskiold-Samøe ApS, for Greenland Environment Research Institute.

Urick, R. J. (1971). The noise of melting icebergs. *The Journal of the Acoustical Society of America, 50*(1B), 337–341.

Urick, R. J. (1984). *Ambient noise in the sea*. Washington, DC: Naval Sea Systems Command, U.S. Department of the Navy.

Vagle, S., Large, W. G., & Farmer, D. M. (1990). An evaluation of the WOTAN technique of inferring oceanic winds from underwater ambient sound. *Journal of Atmospheric and Oceanic Technology, 7*(4), 576–595.

Verrall, R., & Ganton, J. H. (1977). *The reflection of acoustic waves in sea water from an ice covered surface*. Technical Memorandum 77–8. Victoria: Defence Research Establishment Pacific.

Wenz, G. M. (1962). Acoustic ambient noise in the ocean: Spectra and sources. *The Journal of the Acoustical Society of America, 34*(12), 1936–1956.

Worcester, P. F. (2015). *Canada Basin Acoustic Propagation Experiment (CANAPE)*. Technical Report no. AD1013930, Scripps Institution of Oceanography, University of California, San Diego.

Xie, Y., & Farmer, D. M. (1991). Acoustical radiation from thermally stressed sea ice. *The Journal of the Acoustical Society of America, 89*(5), 2215–2231.

Yang, T. C., Giellis, G. R., Votaw, C. W., & Diachok, O. I. (1987). Acoustic properties of ice edge noise in the Greenland Sea. *The Journal of the Acoustical Society of America, 82*(3), 1034–1038.

Ye, Z. (1995). Sound generation by ice floe rubbing. *The Journal of the Acoustical Society of America, 97*(4), 2191–2198.

Zakarauskas, P., Parfitt, C. J., & Thorleifson, J. M. (1991). Automatic extraction of spring-time ambient noise transients. *The Journal of the Acoustical Society of America, 90*(1), 470–474.